

Intelligent PCD Tool Testing and Prediction of Performance



Ramesh Kuppuswamy and Kerry Anne Airey

Abstract The ongoing competition on cutting tools drive the tool manufactures to enhance the cutting tool quality through real-time condition monitoring and performance prediction. The digitization of tool within the manufacturing process, allows for the creation of an intelligent manufacturing system, to reduce the cycle time required for testing, and facilitate the categorization of tool performance as well as early warning signals of the change in the manufacturing processes. The system comprises two platforms such as feature extraction engine (FEE) and feature prediction engine (FPE). The FEE monitors real-time progression of operational behavior during wear with the tool–work interface signals. The accelerated tool wear testing applies a milling arrangement, incorporating a clock-testing workpiece that simulates an intermittent cutting process on hardened steel. The feature extraction engine uses the accelerated wear results to build a calibrated wear model as a reference tool for wear analysis and prediction. Flank wear lands were imaged using a Leica toolmaker’s microscope and used to calibrate the wear model, correlating the digital signal feature to the tool–work interface wear behavior. The imaged wear progression, force, and acoustic emission signal features were analyzed by statistical methods including applications of Spiro-Wilks, ANOVA, and Kruskal–Wallis evaluations. This confirms the experimental accuracy and provides the baseline for wear prediction driving the development of a feature prediction engine (FPE). The results are a significant reduction in the quality control cycle time and performance prediction. The experimental results indicate that the FEE correlates accurately across sensors and progression tracking of abrasive wear in the cutting tools, clearly distinguishing between machining cuts, signal noise, and signal anomalies.

Keywords Cutting tools · PCD · Intelligent tool testing · Tool performance prediction

R. Kuppuswamy (✉) · K. A. Airey
Department of Mechanical Engineering, University of Cape Town,
Cape Town, South Africa
e-mail: Ramesh.kuppuswamy@uct.ac.za

© Springer Nature Singapore Pte Ltd. 2018
S. S. Pande and U. S. Dixit (eds.), *Precision Product-Process Design and Optimization*, Lecture Notes on Multidisciplinary Industrial Engineering,
https://doi.org/10.1007/978-981-10-8767-7_7

Nomenclature

σ_y	Yield strength of the PCD cutting insert (GPa)
μ	Population mean of the test samples
E	Young's modulus of the PCD (GPa)
F_n	Normal force exerted on the workpiece during machining (N)
H_{PCD}	Hardness of the PCD matrix (GPa)
i	Number of data points
K_{IC}	Fracture toughness of the PCD insert (MPa m ^{1/2})
l_c	Cutting distance traversed (m)
l	Number of hidden units
L	Levene's statistic (L)
k	Number of sets from which the data come
m	Work hardening factor
n	Size of the sample
N	Total number of sampled cases
P	Weighted sums in a nonlinear model
s	Standard deviation of the experimental data
t	" t " factor
$V_{abrasive}$	Volume lost from the cutting insert (m ³)
x	Sample mean
w	Neuron weights
Z	Array of the mean and median values of the sampled case i from group j

1 Introduction

The ongoing thrust toward a high value manufacturing and services necessitates the manufacturing industries to ensure total system uptime, reliability, and efficiency, particularly for mission-critical high value assets. Conventional approaches such as scheduled preventive maintenance and reactive "fail-and-fix" methods are no longer adequate or effective to meet the increasingly higher operational availability at an affordable cost. In addition, with a paradigm shift toward "fly by the hour" business models, original equipment, lines, engines, and tools manufacturers (OEMs) are compelled to remodel the traditional ways of maintaining these resources to broaden their revenue streams by providing 100% fulfillment at all time. The problem is severe when the manufacturing processes change the product characteristics in terms of dimensional features, precision, and surface integrity. The cutting tool industries often battle to maintain a consistent quality as the manufacturing process varies continuously. Use of intelligent cutting tool testing and prediction of performance would transform manufacturing into predictive reliability so that a consistent quality can be maintained in the tool manufacturing. One such in-demand technology is the use of polycrystalline diamond (PCD) cutters, as

cutting inserts brazed into oil well drill bits (National Renewable Energy Laboratory 2000). This increasing demand for PCD cutters necessitate research on PCD performance optimization, with the objective of extending tool-life cycles. The process of enforcing high quality standards and real-time modification of the manufacturing process to account for creeping manufacturing defects becomes a critical tool in the production of PCD inserts. Current quality control processes are inadequate, inefficient processes, which do not operate as real-time applications, resulting in excessive time wastage and subquality inserts that must be discarded. Research on intelligent tool testing methods, therefore, becomes a priority, emphasizing digital monitoring of PCD wear behavior and extending to appropriate predictive analysis. The intent being to establish links between the manufacturing process and the failure behavior of the PCD insert. The quality control process associated with the preemptive elimination of these undesirable features, significantly extend the manufacturing time of an insert batch and require extensive hands-on qualitative analysis by experienced personnel. Accelerating the quality control approach would enable faster rectification of nonideal failure mechanisms experienced by the PCD cutting tools. Furthermore, the application of necessary corrective actions on the manufacturing floor becomes significantly faster than current protocols allow. This, in turn, minimizes material wastage and prioritizes superior tool performance prediction strategies. Ensuring PCD tool compliance to industrial standards begins during manufacture and ends during field testing. During and immediately after manufacture, line inspection procedures assess the PCD tools, for obvious damage and dimensional compliance. In general, the tools presenting with edge chipping, micro-grooving, crack formation, and gouge marks are discarded. Minor surface defects, however, are corrected through further applications of grinding and polishing processes.

The objectives of this research are to develop an intelligent PCD tool testing system that clearly establishes the failure characteristics of the PCD cutting inserts, as well as predicting the product performance. This is implemented via (see Fig. 1):

- (A) Feature extraction engine (FEE) with a dashboard interface, and
- (B) A predictive tool-life model for PCD Failure.

The scope of this research extends to:

- Development of an appropriate sensor system (select, acquire, and set up the most appropriate type of sensors, placement locations, fastening methods; types, levels, and extent of sensory data to achieve balance between accuracy and analytical ability).
- Development of a data acquisition system so as to digitize the behavior of the tool–work interface.
- Testing, validation, and selection of the most appropriate time–frequency cutting signals in terms of the sensitivity and repeatability of the tool characterization at the production testing stages.

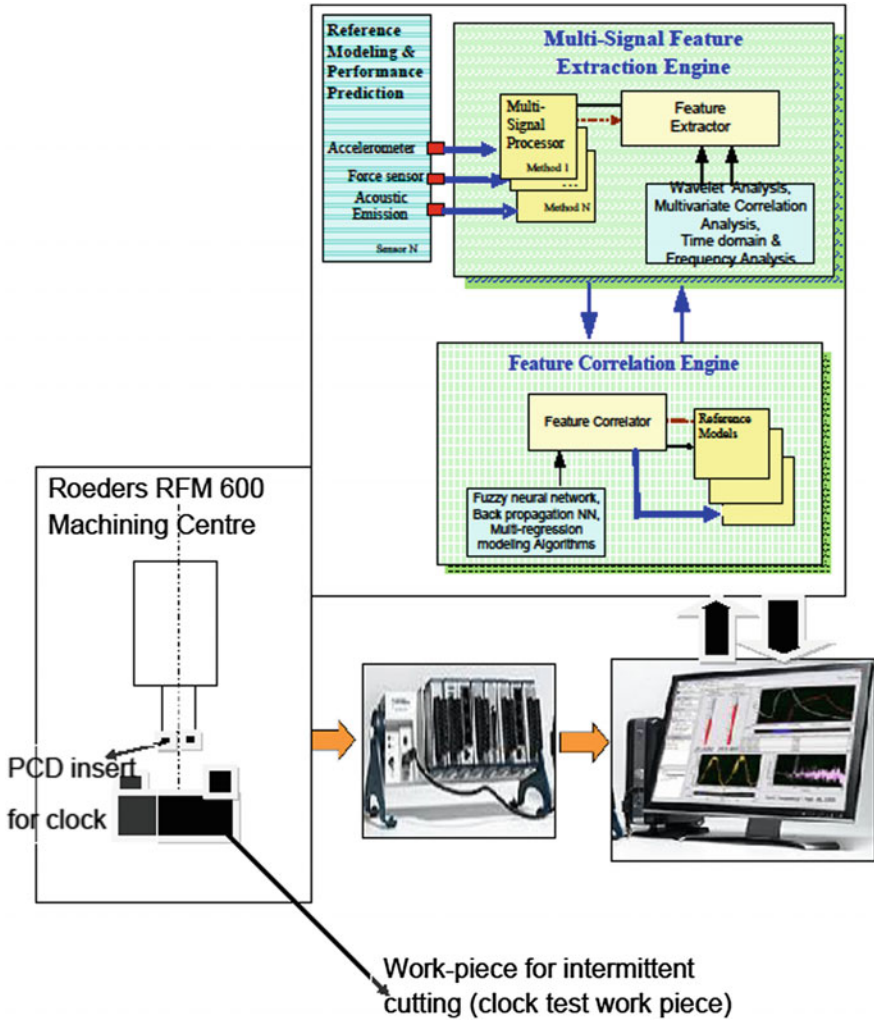


Fig. 1 Plan for development of an intelligent PCD tool testing and prediction of performance

- Testing, validation, and selection of reliable and repeatable feature extraction techniques in the selection of significant parameters for the development of tool-life predictive reference models.
- Testing, validation, and selection of effective self-learning techniques in terms of training sample size, convergence speed, and accuracy in predicting the expected life span of cutters at production testing stages.
- Testing, validation, and selection of the most effective clustering techniques in terms of the accuracy, reliability, and repeatability in mapping specific signals in

relation to known reference models for the prediction of PCD cutting insert life span at production testing stages.

- Distillation of the best sensory signals, feature extraction, learning, and clustering methods for the development of reference models.
- To test the effectiveness of the reference models for the characterization of PCD inserts in a nondestructive and dynamic manner.

2 A Review of PCD Tool Testing Methods

Ensuring PCD compliance to industrial standards begins during manufacture and ends during field testing of the inserts. The testing methods are grouped into industrial-based testing and laboratory-based testing methods as described below.

2.1 *Industrial-Based Testing for PCD Tools*

- **Field testing**

The field tests conducted at the industries predominantly determines the wear progression and evaluate this against performance expectations. This data is unable to isolate the performance behavior of the PCD tool against the manufacturing inputs but collectively addresses the tool, machine, and process characteristics. As a result, the tool manufacturers are unable to impart corrective actions into their production processes. Furthermore, relying on this method is time-consuming and expensive, with excessive equipment requirements and high scrappage anticipated prior to defect correction.

- **Simulated field testing**

A simulated field test is devised to eliminate third parties from the testing process. However, simulated field testing methods are time-consuming and expensive, as they tend to be associated with high levels of tools scrappage. Despite the encompassing nature of the simulated tests, several approximations are needed, and hence, the accuracy of tool testing is compromised.

- **Accelerated tool wear testing**

With the intention of reducing tool testing time accelerated tool wear (ATW) testing protocols are employed by the tool manufacturers but a time-consuming post-mortem analysis is a prerequisite to link the failure characteristics of the cutting tool to the respective manufacturing processes. A typical example of accelerated tool wear testing is shown in Fig. 2.

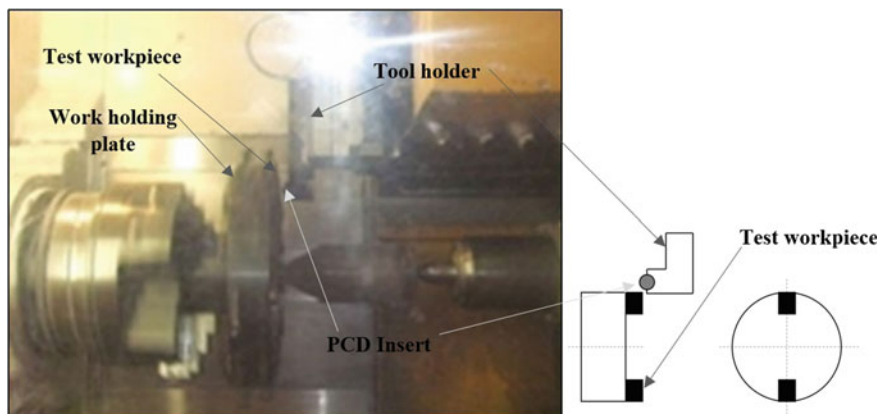


Fig. 2 Accelerated cutting tool testing employed by the cutting tool manufacturers

2.2 Laboratory-Based Testing of PCD Tools

The laboratory approaches to investigating cutting tool product performance are intended to develop an understanding of the failure behavior of a given cutting insert during testing.

- **Nondestructive testing (NDT)**

Nondestructive tests aim to identify and remove from circulation, defective cutting tools prior to conducting destructive tests that focus on identifying and correcting significant insert flaws.

- **Visual inspection**

Visual inspection processes in laboratory settings progress with line operators inspecting the PCD tools as they come off the production line. Scanning electron microscope was used to accurately measure the wear of the diamond-like coatings (Thorwarth et al. 2015). Material properties, including porosity and particle grain size, can be confirmed using SEM analysis, with the added advantage of inspecting the surface for the presence of micro-crack defects, likely to propagate in fracture failure. This analysis is largely unsuited for use in tracking the severity of wear between machining passes, as the time and cost commitment is high. Not all experimental or industrial environments have this equipment available for use. A more economical alternative for monitoring flank wear is a toolmaker's microscope.

- **Raman spectral analysis**

The Raman spectral analysis and applications of ultrasonic tests have had some success in identifying defects especially for the PCD matrix (Radtke 2006). Incomplete matrix mixing and nonuniform material concentration flaws can be

detected, but there are limitations in their ability to locate the vertical positioning of the defect within the matrix layer. Obvious defect detection can help rectify poor quality cutting tools, but cannot assist in identifying those cutting tools without defects that will still underperform. Before and after Raman spectroscopy studies on fatigued oil and gas cutting tools mainly the PCD cutters exhibited changes in the stress field of the matrix, from general compressive stress fields to residual tensile stress fields (Vhareta et al. 2012).

On an overall note, the nondestructive evaluation confirms the cutting tool's material properties and has some success in identifying obvious external, and to a limited degree, internal defects, but is most powerful in providing baseline reference imaging of the cutting tool's surface textures.

- **Destructive testing**

Standard destructive testing protocols, like breakage tests, tend to focus on information obtained at the point of failure. Information that is more pertinent to the evaluation of wear performance is obtained in the moments prior to failure which presents the behavioral changes in the insert, indicative of imminent failure. Common apparatus for testing tool wear are lathe or milling stations. Lathes have the obvious advantage of generally mounting single cutting tools. Khidhir et al. (2015) chose to turn a single point cemented carbide cutting insert, simplifying their analysis and focusing on the creation of the prediction model for product performance. Milling machine applies a wider range of cutting tools and is capable of using multiple insert tool holders. Che et al. (2012) recommend isolating a single cutting insert, to simplify the correlation of machining signals to wear development, and eliminate noises. In this manner, a single cutting insert operating with minimal milling station features can provide a holistic signal representation of insert failure, from initiation through growth to catastrophic termination of the insert.

- **Wear growth analysis**

Most wear analysis bases itself on empirical relations tracks the progression of tool wear against the cutting distance traversed to generate that level of wear (Arsecularatne et al. 2006). Further machining with the same tool-work combination allows tool performance predictions to be calculated from this wear curve. Where new or used tool-work combinations are tested, the algebraic constant parameters developed by the Taylor relation are unlikely to exist in literature. One method of investigating tool wear is to determine these constants during testing. de Mesquita et al. (2011) have demonstrated the Taylor relation method for computing the tool life on turning ABNT 1038. The method tracks the flank wear progression against cutting time to plot a Taylor tool-life curve, and algebraic constants were computed. Using the Taylor relation, further instances of tool life were predicted to plan removal time of the cutting tool from the CNC machining operations. Evaluating these curves for wear behavior shows initially faster wear rates that stabilize to almost constant wear rates, until rapidly generated wear occurs just prior to failure, or alternatively, a catastrophic failure occurs (Kato and Adachi 2001).

Quantifying the extent and severity of wear mechanisms defines the rate of wear generation and the mechanism of insert failure.

- **Flank wear analysis**

ISO standards require that the tool maintain its cutting edge as long as the limit of flank wear not exceeding $VB = 0.3$ mm (Juneja 2005; Palanisamy et al. 2008), at which point the tool is declared worn and substituted for a sharp tool. Standard flank wear is measured linearly down the flank face from the cutting edge to the extremity of the wear land. A marked limitation of this approach is that the position of maximum wear can misrepresent the severity of the wear. Kuttolamadom (2012) suggested taking the average linear wear measurement as the flank wear across a series of points along the flank face, generating more realistic flank wear values. For small flank wear presentations, as with short-cycle quality control tests, this can be challenging to measure with only slight incremental wear rates experienced between passes.

- **Volumetric flank wear analysis**

A past analysis of a volumetric wear approach for the turning TI-6Al-4V with carbide cutting tools, considering the volume of material lost from the cutting tools is a more accurate indicator of the severity of wear. This allows for an accurate three-dimensional representation of the wear land through the cutting tool. Their analysis is driven by the modeling of the dominant microstructural wear mechanism, and its application to predictive modeling. This approach is highly dependent on the process, machine parameters, and tool-workpiece combination (Kuttolamadom 2012). Indeed, Adesta et al. (2010) quantified their simulated flank wear through volumetric analysis during high-speed hard turning. This approach must be customized to both the tool geometry and relative orientation of the cutting plane to describe the extent of his insert wear by integrating over both dimensions of orthogonal cutting process generating a 3D wear volume (Palmai 2014). Unique tool geometries can prove challenging to map as a 3D wear volume and small inaccuracies in the wear measurements can be magnified through calculation of the volume. Burger et al. (2009) used a Zygo NewView 7200 white light interferometer 3D imaging technique to map the worn areas of their titanium milling inserts. This allows them to characterize failure mechanisms for each of the tool edges and complements the unusual geometry of their cutting inserts that incorporate chip breaker features and clamping sites, which would otherwise make modeling the volume of the cutting inserts lost, a lengthy and problematic exercise. Unfortunately, the use of highly specialized imaging software adds time delays and costs to the data processing. 3D mapping should only be applied to those worn areas not easily determined through geometric analysis. Monitoring wear volume during machining cannot be done through imaging, as the wear face will always be in contact with the machining surface. Additional analytical approaches are needed to both categorize the wear mechanism and monitor its development during machining.

- **Tool condition monitoring**

Research by Maropoulos et al. (1996), Arsecularatne et al. (2006) and Byrne et al. (1995) illustrates this point by discussing the vast array of approaches to condition monitoring of cutting tools. Most approaches include indirectly monitoring wear via cutting forces, temperature, vibrations, surface finishes, acoustic emissions, and subsequently building relations between these signals and direct imaging of wear progression through the tool. Byrne et al. (1995), also championed the incorporation of torque, current, power, speed, touch probes, microphones, and smoke sensors. Harnessing this behavior in condition monitoring systems allows accurate, timeous quality control checks to be developed.

Condition monitoring strives for accurate real-time feedback of tool condition. Most investigations begin with dynamometer installations that offer good force/thrust tracking. This sensor offers real-time force monitoring that is independent of cutting conditions and drill geometry (El-Wardany et al. 1995). Ivester et al. (2000) used a Kistler three-axis dynamometer to record the machining forces for various rake angles in turning AISI1045 with coated and uncoated WC/CO Kennametal grade K68 turning inserts. The force comparison to wear land formation generates a calibrated database for changing rake angles. Mandal et al. (2011) used three-axis dynamometers to isolate tangential, radial, and longitudinal forces during lathe boring of Ti6Al4 V and lathe turning of zirconia toughened alumina. Wang et al. (2013) isolated the orthogonal x , y , z forces when milling stainless steel (HRC52) with ball nosed tungsten carbide cutters. Generating force data through dynamometers is an accurate, real-time indication of force increases. Correlating this data to wear generation often requires further data analysis. Wang et al. (2013) used a preliminary off-line calculation to build and calibrate their wear model, with the intent to operate the model in real time thereafter. Additional indirect wear monitoring can be achieved through acoustic emission (AE) sensors and accelerometers. Jemielniak et al. (2008) successfully compared acoustic emission signals to force signals, tracking wear development in micro-milling applications. Here, the change in amplitude from signal mean to signal peak, in both the positive and negative directions was used to “train” their system to recognize wear behavior, after each pass. The signal changes were graphed against the subsequent used tool life (where the used tool life is equal to, the current tool life (in minutes) over the total possible tool life), and approximated using a second-degree polynomial. Focusing on the change in signal was thought to eliminate baseline variations that develop due to uncontrollable variations in cutting conditions, presenting only the most relevant signals features are extracted for wear information (Jemielniak et al. 2008). Govenkar et al. (1996) discussed the applications of AE sensors to nondestructive and destructive testing protocols. AE sensor’s sensitivity to the sudden strain energy propagation of stress waves allow them to be applied to structures surrounding the machining interface, like exposing the acoustic emission sensor to the machining interface via a “jet of cooling fluid” and monitor the machining process. Govenkar et al. (1996) was able to identify the types of chips ejected from the interface, successfully differentiate between spiral chips of 160, 8, and 3 mm in

length, with FFT analysis recording higher amplitudes for shorter chip lengths. Other studies have considered AE sensors mounted indirectly through the cutting fluid and directly seated on either the tool, or workpiece. Inasaki (1998) has established the effective use of AE sensor on capturing chip formation signals regardless of its placement. Furthermore, the AE sensors was effectively used on distinguishing the chip formation signals from the surrounding signals. AE monitoring of turning recorded wear signals isolated from machine vibrations and external vibrations. This is owing to the AE operating frequency range, which falls above the operating vibration frequency of the lathe. In a study comparing the ability of AE sensors, accelerometers, and spectrometric oil analysis to detect pitting wear in spur gears, the AE sensor was the only one responsive enough to distinguish pitting wear in time to remove the gear before performance suffered (Tan et al. 2007). Li (2002) attempted experimental investigations into delamination wear phenomena. The speed at which delamination events occur from the trigger event to the surface separation makes difficulty in prediction of event. The ensuing signal chaos is a secondary contributor, as the delaminated surface interacts with the machining interface, causing damage. Successful tests found that when monitoring the AE signal output in both the frequency and the time domains, it exhibits distinct amplitude drops in the signal output, immediately following delamination events. Ravindra et al. (1997) had success with using their AE sensor to track flank wear, with their rise times resembling rapid run in wear (stage 1 of flank wear), steady wear progression, and finally chipping or catastrophic tool failure. AE sensors offer real-time operation in frequencies that immediately exclude structural resonances and background noise generated by surrounding machines. AE signals are sensitive to wear fluctuations and fracture events, with non-directionality that reduces the number of sensors required. AE sensors are compact and easy to mount, but are largely dependent on the process parameters, with reference wear models requiring experimental calibration before implementation. An alternative to the AE sensor is an accelerometer. Bierman et al. (2013) successfully measured the vibrations in five-axis machining, where the frequency recorded is a multiple of the spindle rotation frequency. Comparing this accelerometer to contact-emission sensors commonly used to tune musical instruments, they found good correlation between sensors, although the positioning of the contact sensor very close to the location of the vibration was necessary to ensure accuracy. The acoustic emission sensor provides reasonably accurate results, regardless of positioning. Fang et al. (2012) found a triaxial accelerometer sensitive enough to track orthogonal vibrations in high-speed machining of Inconel 718, using wavelet analysis and comparing this output to the cutting force data to evaluate the extent of the tool wear. Touch probes are another consistent vibration monitoring option that is easy to implement and rarely requirement machine modifications. Their dependency on specific experimental materials and cutting conditions limits their application to generic wear monitoring, while their low sensitivity limit their applications to monitoring high performance tools (El-Wardany et al. 1995). Analyzing the quality of a machined surface finish is a good indicator of insert cutting performance, but is heavily influenced by tool geometry, cutting speeds, and feed rates. Colding (2004)

suggested that average surface roughness values must be related to tool radius before accurate wear implications can be made. The presence of burr formations (Chen 2005) or material adhesions can indicate that the cutting interface temperature rose too high during machining, implying a worn tool was operated, or nonideal failure occurred. This artificially raises the average surface roughness values, with large peak-to-peaks expected. Ozel and Karpaz (2005) used calibrated models to begin predicting the surface finish after training a neural network with experimental data and monitoring flank wear. They noted that surface finish's reliance on geometric and machining parameters make this difficult to apply to new tool-work combinations (Ozel et al. 2007). Childs et al. (2008), Khidhir et al. (2015) and Kuttolamadom et al. (2015) obtained their experimental average surface roughness parameters using various profilometers, all of which require testing to be conducted post-machining, adding time delays and increasing the personnel requirements for quality testing protocols. Palanisamy et al. (2008) used surface finish to target their optimal cutting conditions before beginning to build their tool wear prediction model. Surface finish used in this manner could help identify accelerated wear testing conditions designed to reduce the testing cycle for quality control processes. A final method of directly determining the influence that wear generation in cutting tools has on the machining process is to measure the increase in temperature at the cutting interface during each successive cutting pass and establishing relations between this temperature behavior and the quantity of wear presenting in the tool. During the turning of AISI 1045 with coated and uncoated WC/Co inserts, Ivester et al. (2000) incorporated thermocouples into the bi-conducting tool-chip interface, operating as the junction for the thermocouple and tracking the voltage readout. The results of which were lower amplitude variations than produced across force signatures and insufficient data from the coated inserts. Thermocouples are time-consuming to embed into the workpieces and cannot necessarily be mounted close enough to the machining interface. Thermal cameras providing real-time temperature evaluation must be positioned in line-of-sight of the cutting interface without forward protective barriers. Lin and Ting (1995), among others, noted that placement of sensors in the appropriate orientation and correct proximity to the cutting interface are vital to obtain precise experimental results. El-Wardany et al. (1995) commented that it would further reduce the impact of noisy signals, and false alarms generated by natural frequencies of the spindle and motor within the machine. This can present positioning challenges in close machining or drilling environments, where tools are expected to bore down into or through workpiece materials, while the monitoring system is expected to continue to operate.

One commonality through the research so far is that it mostly pertains to flank wear, although Lu and Chou (2011) considered on delamination failure events. The designer of quality control tests should be mindful that at some point, inferior tools failing by nonideal wear mechanisms will pass through the evaluation. The system must be able to handle, identify, and alert the operator to the discovery of nonideal fracture failure of the PCD tool. Table 1 summarizes the past PCD tool testing methods

Table 1 PCD tool testing methods

PCD tool testing method	Principle	Advantages	Shortfalls	Reference
Industrial approach	Field testing	Reasonably accurate	Difficult to identify the exact source of failure	Huges (2014)
Industrial approach	Simulated field tests	Reasonably accurate	Difficult to identify the exact source of failure	Huges (2014)
Visual inspection	SEM analysis	Enable to identify the grain size, porosity, and micro-cracks	Lack of information on wear resistance and strength	Thorwarth et al. (2015)
Raman spectral analysis	Optical test	Enable to identify the defects with the PCD matrix	Difficult to establish the internal defects of PCD	Radtke (2006) and Vhareta (2012)
Machining test	Continuous turning	Enable to establish the wear resistance in the form of flank wear	Consumes enormous time as the PCD tool has to undergo an image analysis to understand its failure characteristics	Khidhir et al. (2015)
Machining test	Process parameters study	Enable to establish the wear generation phenomenon	It is equivalent to a postmortem study and consumes time	Byrne et al. (1995)
Condition monitoring	Process parameters study using dynamometers	Accurate	Suitable only for the laboratory	El-Wardany et al. (1995)
Condition monitoring	Process parameter study using AE sensors	Less expensive method	Erratic results at times of delamination	Li (2002)

The PCD tool testing methods described in Table 1 are centered on in-process manufacturing tests and consume time. As a result, the scrap rate of PCD tools between the time of fault finding and corrective action on the production floor is high. Therefore, intelligent approaches were applied to estimate tool wear states. Application of neural networks (NN) and clustering techniques such as multilayer perceptron (MLP), adaptive resonance networks (ART2), support vector machine (SVM), and self-organizing maps (SOM) was attempted for establishing the tool wear maps (Si et al. 2011). Also, hidden Markov models (HMM) were successfully applied as it represents the temporary signal dynamics and reasoning in speech recognition. These methods were used for prognostic evaluation of tool wear, finding 92.5% experimental compliance with wear signals (Zhu et al. 2009). A major limitation of these methods is its lack of consideration on fracture failure mechanisms. Intelligent tool testing systems that did not handle the fracture events

tend to limit the real-time quality control processes. Research on intelligent tool testing methods, therefore becomes, a priority, emphasizing digital monitoring of PCD wear behavior and extending to appropriate predictive analysis. Accelerating the quality control approach would enable faster rectification of nonideal failure mechanisms experienced by the inserts. Furthermore, the application of necessary corrective actions on the manufacturing floor becomes significantly faster than the current protocols allow. This, in turn, minimizes the material wastage and prioritizes the PCD life prediction strategies. Therefore, the objectives of this project are to develop an intelligent PCD insert clock-testing system that clearly establishes the failure characteristics of the PCD cutting inserts, as well as predicting the product performance.

3 Experimental Setup

The machining experiments were conducted on Rödgers RFM 600 high-speed machining center using a PCD milling cutter head over a linear clock-testing workpiece as illustrated in Fig. 3. Throughout the experiments, the force signatures were captured and amplified, and further analysis was done using the data acquisition software Dewesoft, to understand the tool–work interface behavior. Every cutting experiment was repeated five times, and the average cutting forces of at least three tests with the clearest values were taken. The machined workpiece surface texture was examined using a scanning electron microscope (SEM) and the surface roughness was examined using a Surtronic profilometer. After every 5 m of cutting distance, the flank wear was measured using a tool maker’s microscope. The AE sensor tracks machine frequencies above 10 Hz, while the dynamometer x , y -directions track forces from -10 kN up to 10 kN. The z -direction has 15 kN upper and lower limits. The temperature at the cutting interface was estimated by assessing the color of the sparks generated during testing and comparing these to the known glow point of silver steel. The accelerometer was calibrated using a Rion VE10 vibration generator.

This milling cutter head was configured to hold a PCD insert of size D16 \times 12 mm at a negative rake angle and mounted on HSK 40 tool holder. The milling conditions for performing the machining test are given in Table 2.

4 Results and Discussion

The experimental results have enabled to create a quality control approach that analyzes PCD insert cutting performance, with a view to incorporating accelerated wear generation and combining this with intelligent condition monitoring in order to predict the product performance. The results include the output of extensive experimental findings and its signal correlation with the flank wear behavior.

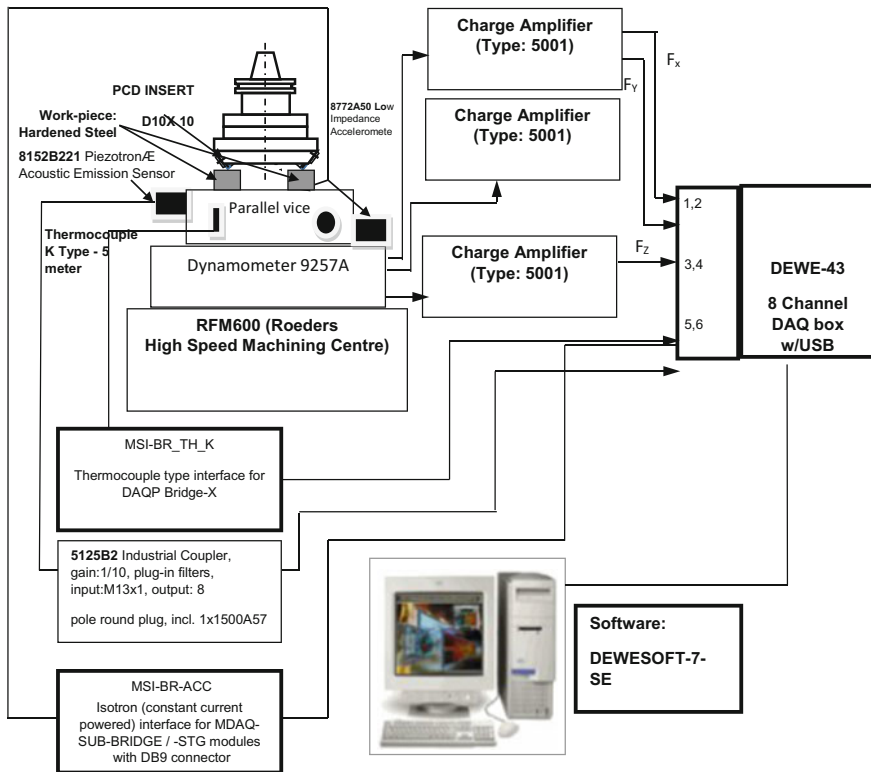


Fig. 3 Experimental setup and data acquisition arrangement for the machining experiments

Table 2 Milling conditions for the accelerated wear tests

Detail	Unit	Value
Milling type	–	Intermitted cutting (clock testing)
Cutting speed	m/min	534.2
Feed rate	mm/min	1200.00
Depth of cut	mm	0.05
Material removal rate	mm ³ /min	60.00
PCD insert size	mm/mm	D16 × 12
Workpiece material and hardness	–	Medium carbon alloy steel and HRC 45

Furthermore, ANOVA analysis was performed for validating the AE sensor signatures, and neural network analysis was done to find the performance prediction of the PCD inserts.

4.1 Flank Wear

Flank wear is the gradual, consistent loss of material from a cutting tool, which degrades the cutting edge and distorts the tool geometry. Flank wear is usually characterized by abrasion, sudden catastrophic failure and brittle fracture of a PCD insert, and the growth of flank wear indirectly explains the physical properties of a PCD insert such as wear resistance and transverse rupture strength. In order to distil the effect of built-up edge formation, volumetric flank wear, and VB, accelerated wear tests were performed, and the results are shown in Figs. 4 and 5. In general, the localized cracking around diamond grains or failure of the binding matrix will also result in the smallest diamond particles becoming loose and falling out during machining. All of these effects combine in the abrasion wear of a PCD insert as shown in Fig. 6.

Using the PCD material information, the following relationship for the calculation of volumetric wear under abrasive wear mechanisms is presented by Stolarski (2000):

$$V_{\text{abrasive-theoretical}} = \frac{m^2 * \sigma_y * E * F_n^{3/2} * l_c}{K_{IC}^2 H_{PCD}^{3/2}} \tag{1}$$

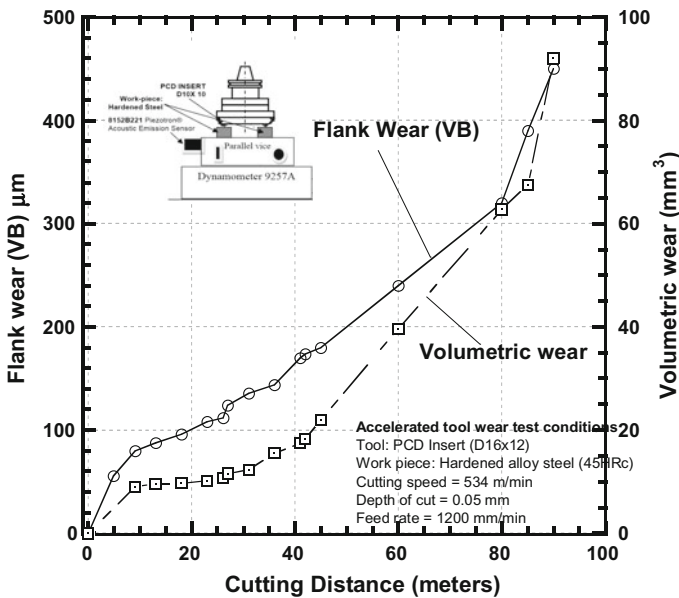


Fig. 4 Flank wear behavior of a PCD insert at accelerated tool test conditions

V_{abrasive} represents the volume lost from the cutting insert (m^3), while m is the work hardening factor, equated to the workpiece hardness over cutting insert hardness. σ_y , is the yield strength (GPa) of the cutting insert, of PCD owing to its nature as a brittle material, E is Young's modulus (GPa) for PCD, F_n is the normal force (N) exerted on the workpiece during machining and l_c is the cutting distance (m) traversed. K_{IC} , denotes the fracture toughness ($\text{MPa m}^{1/2}$) experienced by the PCD material and finally H_{PCD} represents the hardness (GPa) of the PCD matrix.

Abrasion wear volume can be corroborated through direct imaging and measurement of the wear region under a toolmaker's microscope. Post-machining weigh-ins can be conducted, comparing the final worn PCD insert weight to the weight of the insert prior to machining, and calculating the volume of the lost material based on the density of the PCD material matrix. This does become slightly more complicated once the WC-Co base becomes involved in wear mechanisms, however, the use of accelerated wear testing protocol should limit wear to the PCD matrix. Geometric analysis can model the volume of PCD material lost from a theoretically ideal cutting insert, by assuming the PCD cutting inserts as a simple cylindrical shape with an inclined wear plane. In this manner, the lost volume would approximate a cylindrical wedge tracks the progression of the wear from zero to a completely used insert as the inclined machining interface progresses through a PCD insert (Fig. 7).

By considering the geometrical form of the worn portion of the PCD tool, the volumetric wear is given as

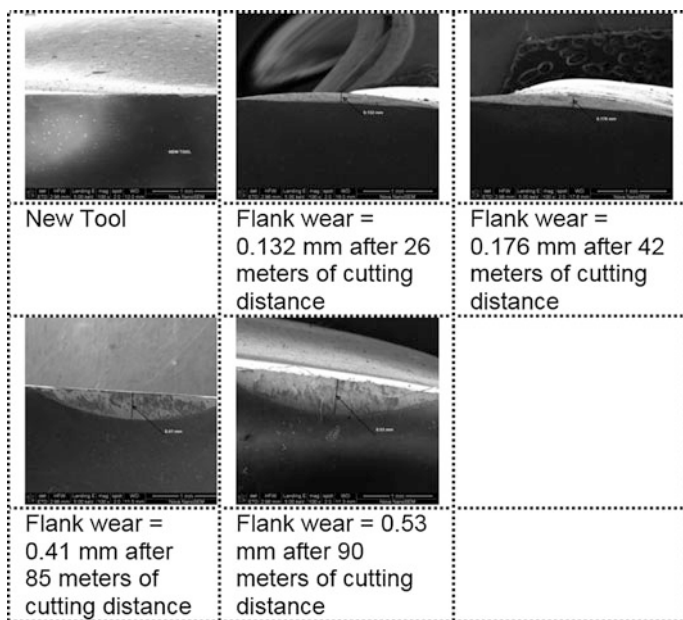


Fig. 5 Flank wear images of a PCD insert at accelerated tool test conditions

Fig. 6 Geometric arrangement of volumetric abrasion wear determination

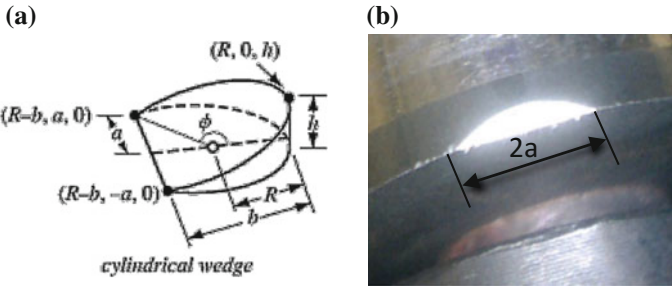
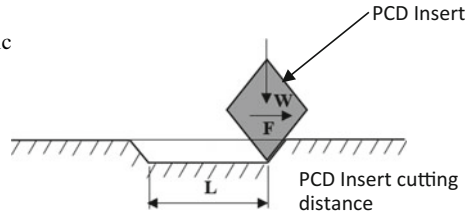


Fig. 7 Dimensional correlation for volumetric wear computations, **a** theoretical model and **b** actual wear

$$V_{PCD} = \frac{hR^2}{3} \left[\frac{3 \sin \theta - 3\theta \cos \theta - \sin 3\theta}{1 - \cos \theta} \right] \tag{2}$$

The values for a , b , h , and θ was obtained from the PCD worn insert image as it corresponds to dimension $2a$ indicated on the flank wear image (Fig. 7b) (Wolfram Math World 2013) (see Appendix 1 for more details).

• **Wear modeling and signal interrelations**

The tool–work interface conditions were monitored in terms of cutting forces, acoustic emission signals, and correlated with the flank wear growth behavior of the PCD cutting inserts. Specific relationships between these signals and the cutting distance were established using the data-driven models. The developed data-driven model was applied to predict the remaining useful life of the PCD tool. Shown in Fig. 8 is the behavior of cutting forces and AE_{RMS} signals for the PCD tools at various cutting distances. The cutting forces behavior suggests that as the cutting distance increases the cutting forces increases consistently with each cutting pass until a maximum force is reached. Continuing machining resulted in an additional signal spike and beyond this signal, the failure of the PCD insert was apparently seen. Between the cutting distances from 0 to 30 m, the increase in cutting forces was found to be higher than the cutting distance range 30–80 m. AE_{RMS} has exhibited a similar trend and confirms the suitability of using AE_{RMS} signals as a measure of cutting forces and flank wear growth behavior.

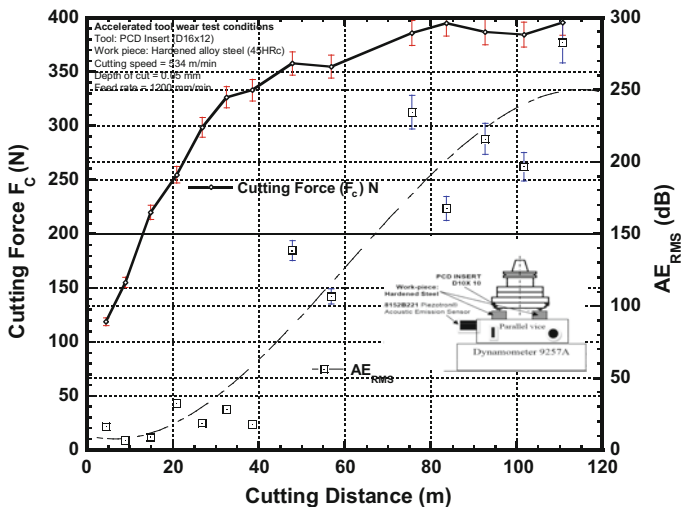


Fig. 8 Cutting forces and AE_{RMS} behavior for various cutting distances

• ANOVA analysis

To further demonstrate the correlation between force signals and AE sensor signals, ANOVA tests were performed. As a result, the dynamic digitized map of the tool–work interface signals of the reference samples was clearly sketched inclusive of errors and variation. Shown in Table 3 are the experimental results of cutting forces and AE_{RMS} signals for various cutting distances.

Table 3 Variables factors of the experiments and results

Cutting conditions	Cutting distance (m)	Cutting force F_c (N)	AE_{RMS} (dB)	Flank wear (μm)
Fixed cutting conditions: intermittent cutting (clock testing); cutting speed = 534.2 m/min; feed rate = 1200.00 mm/min; depth of cut = 0.05 mm; material PCD insert: D16 × 12	4.8	118.78	16.344	56
	9	154.99	6.7500	80
	13	219.96	8.9300	88
	18	254.56	32.688	96
	23	298.33	18.910	108
	27	326.22	28.370	124
	31	332.85	17.920	136
	36	357.57	138.48	144
	41	354.54	106.64	170
	45	385.61	234.38	180
	60	394.81	167.57	240
	80	386.49	215.82	320
	85	384.08	196.54	390
	90	395.45	282.44	450

The cutting force (F_c) is the resultant of the measured forces F_x , F_y , and F_z . AE_{RMS} signals were measured at the nearest point of machining zone as the AE sensor was mounted on the workpiece. In each machining experiment, five sample signals of F_x , F_y , F_z , and AE_{RMS} were taken, and F_c and AE_{RMS} values were computed. The columns F_c and AE_{RMS} shown in Table 3 indicate the mean value of F_c and AE_{RMS} of each experiment. A one-way ANOVA test was applied to compare the effect of a single factor on the different groups: cutting force (F_c) and AE_{RMS} signals. The findings of ANOVA comparison tests on (i) cutting force and flank wear, and (ii) flank wear and AE_{RMS} are shown in Tables 4 and 5, respectively.

The p -values of the parameters resulted from the ANOVA are presented in Tables 4 and 5. The smaller the p -value, the smaller the probability of making mistakes by rejecting the null hypothesis, and consequently, the larger the corresponding coefficient. By evaluating the p -values of the parameters: cutting force signatures and AE_{RMS} signatures, it is found that the cutting force with the p -values smaller than 0.05 exhibits a larger effect on the flank wear than AE_{RMS} signatures. Also, the p -values for AE_{RMS} signatures show the correlation between the cutting force and AE_{RMS} signatures and suggest that the flank wear growth can be studied by both cutting force and AE_{RMS} signatures with reasonable accuracies. Tables 4 and 5 also give the F -value which is the ratio of the groups' mean square over the error mean square. As the value on both cases was found to be more than 1, it suggests that the samples were drawn from a different population although the measurement of AE_{RMS} signals is closest to the cutting zone whereas the cutting forces are the measurement at the cutting zones. The F -values computed using the t -test for the unpaired groups (i) cutting force and flank wear (ii) AE_{RMS} and flank wear was found to be 1.775 and 1.518, respectively. Also, the homogeneity of variance was tested in SPSS by applying the Levene's statistic for nonparametric data (NIST 2014). If the significance p , of statistic L , remains above 0.05, for a 95%

Table 4 ANOVA comparison tests on cutting force and flank wear

Source of variation	Cutting force F_c (N) and flank wear				
	DF	Seq SS	AdjMS	F	p
In between	1	113,442	113,442	9.8	0.004
Within	26	300,923	11,573		
Total	27	414,365	15,346		

Table 5 ANOVA comparison tests on AE_{RMS} and flank wear

Source of variation	AE_{RMS} and flank wear				
	DF	Seq SS	AdjMS	F	p
In between	1	44021.0	44021.0	3.58	0.06
Within	26	319,235	12,278.2		
Total	27	363,256	13453.9		

confidence interval, indicating no significant variation in the data for all inserts, the homogeneity assumptions for comparative analysis would be satisfied. The Levene's statistic (L) equation is given as (NIST 2014)

$$L = \frac{(N - k) \sum_{i=1}^k N_i (Z_i - Z)^2}{(k - 1) \sum_{i=1}^k \sum_{j=1}^{N_i} (Z_{ij} - Z_i)^2} \quad (3)$$

where k represents the number of sets from which the data come, N is the total number of sampled cases, and Z is an array of the mean and median values of the sampled case i from group j . The test values for homogeneity of variance in PCD wear data, using the Levene's statistic was found to be, 0.299, 0.070, 0.952, 0.763, and 0.564 for PCD Insert #1 to Insert #5, respectively. Analyzing the value of the p factor shows no datasets of particular significance, with all p factors consistently above 0.05 in value. As a result, the homogeneity of variance is consistent across all experimental data from PCD cutting inserts, #1 to #5, and satisfies that the data be drawn from population exhibiting equal variance. A similar Levene's test on data: cutting forces (F_c) and AE_{RMS} signals also conclude that the data were drawn from population exhibition equal variances.

- ***t*-test**

The “ t ” factor analysis assesses the variability of the data within each machining cycle. The distribution of the data points within each pass is normally distributed, and the “ t ” factor analysis can be applied directly. The “ t ” factor is computed using Eq. 2 as (IBM 2015)

$$t = \frac{(x - \mu)}{(s/\sqrt{n})} \quad (4)$$

where x is the sample mean, and the population mean is denoted by μ , with “ s ” being the standard deviation, and finally, n represents the size of the sample. The “ t ” factor for each distinct machining pass for the PCD tool is presented in Fig. 9

The cutting force “ F_c ” and “ t ” factor for F_c were tracked against the flank wear, which shows the general correlation between the two, and enable to quantitatively express the cutting force signatures as a wear. On a similar note, the AE_{RMS} signals and t -factor for AE_{RMS} have a correlation with the flank wear growth and doubly confirm the use of AE_{RMS} signals as a measure of flank wear. The same was also expressed quantitatively in terms t_{AE-RMS} factor.

4.2 Frequency Domain Analysis

Between the cutting distance from 5 to 80 m the frequency signal spikes occur at $f = 48, 97$ Hz, for both the AE_{RMS} and cutting force (F_c) signals. However, beyond 80 m of cutting distance, the frequency signals spikes occur at 45, 95, and 190 Hz confirming the significant flank wear of the PCD tool.

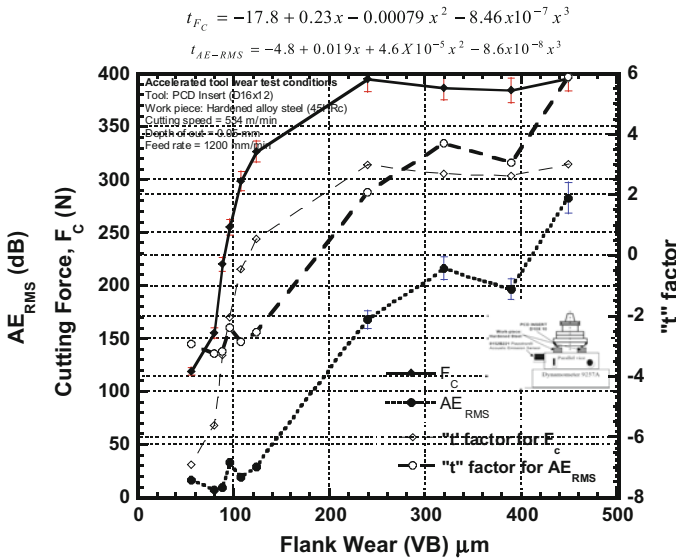


Fig. 9 Cutting force F_c and AE_{RMS} behavior in terms of “ t ” factor

4.3 Predictive Model Generation

Analyzing the signal relationships through multivariate analysis has enabled to build the neural network and a wear model using the machining variables (Liu and Jolley 2015). Shown in Fig. 10 is the PCD wear multilayer perceptron using the neural network architecture.

The hidden layer tracks the data bias between outputs and is used to evaluate the influence of the inputs through weighted sums in a nonlinear model as detailed in Eq. 3 (IBM 2015).

$$P = \sigma \left\{ \sum_{i=1}^l \lambda_i \sigma(x.w_i) \right\} \tag{5}$$

where l equates to the number of hidden units, the sigmoidal function is given as $\sigma(x) = 1/(1 + \exp(-x))$, such that x are the input covariates and “ w ” refers to the neuron weights. The number of data points then becomes “ i ”. The bias term is defined by $x.w_i \underline{\text{def}} \sum_k x_k w_{ik} + w_{io}$. The input covariates for this model are the machining signals identified such as cutting force signatures and acoustic emission signatures.

The neural network architecture uses a single hidden layer with real-time data training to update the synaptic weight after each data record, until the stopping criteria are met. The training criteria for stopping is set as no more than a consecutive step with no error decrease before the algorithm halts itself. Table 6 shows

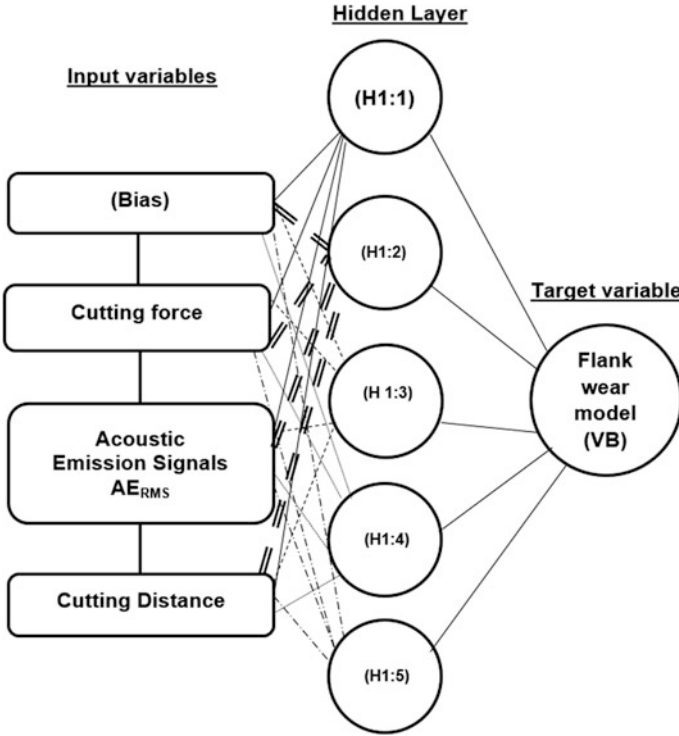


Fig. 10 PCD wear multilayer perceptron using the neural network architecture

the summary of neural network model. The assessment of the model accuracy shows a 6.472 compliance under sum-of-squares methodology creating a 0.087% relative error. The outcome of the neutral network training is an estimation of the model parameters defining the relation between the machining signals variables, the hidden layer, and the wear formation on the PCD cutting insert. These parameters are summarized in Table 7. Understanding the significance of each machining parameter on the magnitude of the wear is critical to ensure the correct emphasis of the variable. Calculating the weighted sum for each of the covariates quantifies their influence on the target variable is given by the following equation (IBM 2015):

$$w_j(x) = \sum_{i=1}^l \lambda_i \sigma'(x.w_i) w_{ij} \tag{6}$$

where the sigmoidal function is given as $\sigma(x) = 1/(1 + \exp(-x))$, such that x are the input covariates and w refers to the neuron weights. The number of data points then becomes i , the bias term is defined by $x.w_i \underline{\text{def}} \sum_k x_k w_{ik} + w_{i0}$, and lambda is the constant term for the data position. Furthermore, the neural network identifies that cutting distance followed by cutting force and acoustic emission signals are the

Table 6 Neural network model summary

Training	Sum-of-squares error	6.472
	Relative error	0.087
	Stopping rule used	1 consecutive step(s) with no decrease in error ^a
	Training time	0:00:00,03
Testing	Sum-of-squares error	2.165
	Relative error	0.058

a excluding the bias unit

Table 7 Neural network estimation of parameter relations: output layer parameter estimates

Predictor		H(1:1)	H(1:2)	H(1:3)	H(1:4)	Predicted hidden layer (H1:5)
Input layer	(Bias)	-0.092	0.951	0.922	-0.141	0.358
	Cutting force	-0.2	-0.522	1.054	-0.172	0.433
	Acoustic emission	0.213	-0.093	-0.037	0.397	0.439
	Cutting distance	0.161	1.086	0.265	0.07	0.409
Output layer: flank wear		-0.706	1.645	0.096	-0.236	-0.426

significant factors of weightage 100, 29.8, and 24.3%, respectively. The imaged flank wear experienced by the PCD inserts during testing are graphed against cutting distance in Fig. 3. The sensor array data signals were modeled against progressive cutting distances and the project values for the cutting force and acoustic emission signals occurring at 80 m of cutting distance and above and projected to be 410 N and 45.05 Hz, respectively.

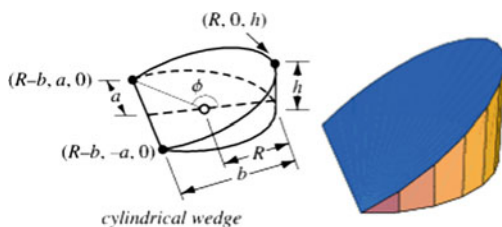
5 Conclusions

This investigation confirms that the developed intelligent PCD clock-testing method enables to evaluate the PCD insert performance in real time. The feature extraction coupled with statistical evaluation along with the neural network training of a predictive model has become an incredibly powerful performance predictor. Once the calibrated model was developed, the DAQ was automated, with the resulting cycle time reducing to approximately 1 min and 40 s for a complete destructive test and real-time calculation of the insert performance relative to the calibrated wear models for a single polycrystalline diamond cutting insert. This represents a noticeable reduction of quality control cycle times, with the actionable feedback produced in real time to be passed to manufacturing production lines. The

accelerated wear test protocol generates representative wear behaviors in the PCD insert, where abrasive flank wear and one instance of insert chipping failure mechanisms were noted without degrading the tool through graphitization mechanisms. Despite the limited fracture events, anecdotal evidence suggests that the sensor array is sensitive enough to extract meaningful signal features from these events, should they occur. Statistical analysis of the data improves the accuracy of the wear models and allows predictive modeling of the flank wear. The strength of this system lies in its ability to effect analysis in real time and its proposed cross-application portability.

Acknowledgements The authors wish to thank Mr. Jonathan Waite University of Cape Town, Cape Town, South Africa for the important contributions made to this research in the initial PCD clock-testing experiments. Further thanks go to Element 6 for the supply of PCD inserts and AE sensors. This project was supported by fund NRF Grant: Incentive Funding for Rated Researchers (IPRR)–South Africa through Reference: IFR150204113619 and Grant No: 96066.

Appendix 1: Computation of Volumetric Wear Using the Principles Cylindrical Wedge



A wedge is cut from a cylinder by slicing with a plane that intersects the base of the cylinder. The volume of a cylindrical wedge can be found by noting that the plane cutting the cylinder passes through the three points illustrated above (with $b > R$), so the three-point form of the plane gives the equation

$$\begin{vmatrix} x & y & z & 1 \\ R - b & a & 0 & 1 \\ R - b & -a & 0 & 1 \\ R & 0 & h & 1 \end{vmatrix} = h(R - b - x) + bz$$

Solving for z is given as

$$z = \frac{(h)(x - R + b)}{b}$$

The value of “a” is given as

$$a = \sqrt{(R^2)((b - R)^2)}$$

$$a = \sqrt{b(2R - b)}$$

The volume of cylindrical wedge is given as the integral of rectangular areas along the x -axis

$$z = \int Z(x)y(x) dx$$

$$Z = \int_{R-b}^R \frac{h(x - R + b)}{b} \sqrt{(R^2 - x^2)} dx$$

$$z = \frac{h}{6b} \left[2\sqrt{(2R - b)b}(3R^2 - 2ab + b^2) - 3\pi R^2(R - b) \sin^{-1} \frac{(R - b)}{R} \right]$$

$$a = R \sin \theta; \quad b = R(1 - \cos \theta); \quad b^2 = 2bR - a^2$$

Hence, $V = \frac{2}{3}hR^2$.

References

- Adesta, E., M. Al Hazza, M.A. Riza, and R. Rosehan. 2010. Tool life estimation model based on simulator tool wear during high speed hard turning. *European Journal of Scientific Research* 39: 265–278.
- Arsecularatne, J., L. Zhang, and C. Montross. 2006. Wear and tool life of tungsten carbide, PCBN and PCD cutting tools. *International Journal of Machine Tools and Manufacture* 46: 482–491.
- Bierman, D., A. Zabel, T. Bruggemann, and A. Barthelmey. 2013. A comparison of low cost structure-borne sound measurement and acceleration measurement for detection of workpiece vibrations in 5-axis simultaneous machining. *CIRP* 12: 91–96.
- Burger, U., M. Kuttolamadom, A. Bryan, and L. Mears. 2009. Volumetric flank wear characterization for titanium milling insert tools. In *Indiana: Proceedings of the 2009 ASME International Manufacturing Science and Engineering Conference*.
- Byrne, G., D. Dornfeld, I. I., G. Ketteler, W. König, and R. Teti. 1995. Tool condition monitoring (TCM)—the status of research and industrial application. *Annals of the CIRP* 44: 541–567.
- Che, D., P. Han, P. Guo, and K. Ehmann. 2012. *Issues in polycrystalline diamond compact cutter-rock interaction from a metal machining point of view-part II: Bit performance and rock cutting mechanics*, 134. JMSE: ASME.
- Chen, G.-L. 2005. Development of a new and simple quick-stop device for the study on chip formation. *International Journal of Machine Tools and Manufacture* 45: 789–794.
- Childs, T., K. Sekiya, R. Tezuka, Y. Yamane, D. Dornfeld, D.-E. Lee, and P. Wright. 2008. Surface finishes from turning and facing with round nosed tools. *CIRP Annals—Manufacturing Technology* 57: 89–92.
- Colding, B.N. 2004. A predictive relationship between forces, surface finish and tool-life. *CIRP Annals* 53: 85.

- de Mesquita, N., J. de Oliveira, and A. Ferraz. 2011. Life prediction of cutting tool by the workpiece cutting condition. *Advanced Materials Research* 223: 554–563.
- El-Wardany, T., D. Gao, and M. Elbestawi. 1995. Tool condition monitoring in drilling using vibration signature analysis. *International Journal of Machine Tools and Manufacture* 36 (6): 687–711.
- Fang, N., P. Pai, and N. Edwards. 2012. Tool-edge wear and wavlet packet transform analysis in high-speed machining of Inconel 718. *Journal of Mechanical Engineering* 58: 191–202.
- Govekar, E., P. Muzic, and I. Grabec. 1996. Classification of chip form based on AE analysis. *Ultrasonics* 34: 467–469.
- Hughes, Baker. 2014. <https://www.bakerhughes.com/products-and-services/drilling/drill-bit-systems/pdc-bits>.
- IBM. 2015. *IBM SPSS neural networks*.
- Inasaki, I. 1998. Application of acoustic emission sensor for monitoring machining processes. *Ultrasonics* 36: 273–281.
- Ivester, R., M. Kennedy, M. Davies, R. Stevenson, J. Thiele, R. Furness, and S. Athavale. 2000. Assessment of machining models: Progress report. *Machining Science and Technology* 4 (3): 511–538.
- Jemielniak, K., S. Bombinski, and P. Aristimuno. 2008. Tool condition monitoring in micromilling based on hierarchical integration of signal measures. *CIRP Annuals—Manufacturing Technology* 57: 121–124.
- Juneja, B. 2005. *Fundamentals of metal cutting and machine tools*, 2nd ed, 134. New Delhi: New Age International (P) Limited Publishers.
- Kato, K., and K. Adachi. 2001. *7: Wear mechanisms*. Boca Raton: CRC Press LLC.
- Khidhir, B., W. Al-Oqaiel, and P. Kareem. 2015. Prediction models by response surface methodology for turning operation. *American Journal of Modelling and Optimization* 3 (1): 1–6.
- Kuttolamadom M. 2012. *Prediction of the wear and evolution of cutting tools in carbide/Ti–6Al–4V machining tribosystem by volumetric tool wear*. Tigerprints.
- Kuttolamadom, M., M. Laine Mears, and T. Kurfess. 2015. The correlation of volumetric wear rate of turning tool inserts with carbide grain sizes. *ASME Journal of Manufacturing Science and Engineering* 137: 011015.
- Li, X. 2002. A brief review: Acoustic emission method for tool wear monitoring during turning. *machine tools & manufacture* 42: 157–165.
- Lin, S., and C. Ting. 1995. Tool wear monitoring in drilling using force signals. *Wear* 180: 53–60.
- Liu, T.-I., and B. Jolley. 2015. Tool condition monitoring (TCM) using neural networks. *International Journal of Advanced Manufacturing Technology* 78: 1999–2007.
- Lu, P., and Y. Chou. 2011. *Analysis of acoustic emission signal evolutions for monitoring diamond-coated tool delamination wear in machining*. Tuscaloosa: University of Alabama.
- Mandal, N., B. Doloi, B. Mondal, and R. Das. 2011. Optimisation of flank wear using Zirconia Toughened Alumina (ZTA) cutting tool: Taguchi method and regression analysis. *Measurement* 44: 2149–2155.
- Maropoulos, P., and B. Alamin. 1996. Integrated tool life prediction and management for an intelligent tool selection system. *Journal of Materials Processing Technology* 61: 225–230.
- National Institute of Standards and Technology. 2014. *Levene test for equality of variances*. www.itl.nist.gov/div898/handbook/eda/section3/eda35a.htm.
- National Renewable Energy Laboratory. 2000. *Diamond-cutter drill bits*. www.nrel.gov/docs/fy00osti/23692.
- Ozel, T., and Y. Karpaz. 2005. Predictive modeling of surface roughness and tool wear in hard turning using regression and neural networks. *International Journal of Machine Tools and Manufacture* 45: 467–479.
- Ozel, T., Y. Karpaz, L. Figueria, and J. Davim. 2007. Modelling of surface finish and tool flank wear in turning of AISI D2 steel with ceramic wiper inserts. *Journal of Materials Processing Technology* 189: 192–198.

- Palanisamy, P., I. Rajendran, and S. Shanmugasundaram. 2008. Prediction of tool wear using regression and ANN models in end-milling operation. *International Journal of Advance Manufacturing Technology* 37: 29–41.
- Palmai, Z. 2014. A new physically defined equation to describe the wear of cutting tools. *ANNALS of Faculty Engineering HUenedoara-International Journal of Engineering* 12: 113.
- Radtke, R. 2006. *New high strength and faster drilling TSP diamond cutters*. Kingwood: Technology International Inc.
- Ravindra, H., Y. Srinivasa, and R. Krishnamurthy. 1997. Acoustic emission for tool condition monitoring in metal cutting. *Wear* 212: 78–84.
- Si, X.S., W. Wang, C.H. Hu, and D.H. Zhou. 2011. Remaining useful life estimation—a review on the statistical data driven approaches. *European Journal of Operational Research* 213 (1): 1–14.
- Si, X.S., W. Wang, C.H. Hu, M.Y. Chen, and D.H. Zhou. 2013. A wiener-process-based degradation model with a recursive filter algorithm for remaining useful life estimation. *Mechanical Systems and Signal Processing* 35 (1–2): 219–237.
- Stolarski, 2000. *Tribology in machine design*, 1st ed. Oxford: Butterworth Heinemann.
- Tan, C., P. Irving, and D. Mba. 2007. A comparative experimental study on diagnostic and prognostic capabilities of acoustic emission, vibration and spectrometric oil analysis for spu gears. *Mechanical Systems and Signal Processing* 21 (1): 208–233.
- Thorwarth, K., G. Thorwarth, R. Figi, B. Weisse, M. Stiefel, and R. Hauert. 2015. On interlayer stability and high-cycle simulator performance of diamond-like carbon layers for articulating joint replacements. *International Journal of Molecular Sciences* 15: 10527–10540.
- Vhareta, M., R. Erasmus, and J. Comins. 2012. Use of Raman spectroscopy to study fatigue type processes on polycrystalline diamond (PCD). In *Durban: 18th World Conference on Nondestructive Testing*.
- Wang, J., P. Wang, and X. Gao. 2013. Tool life prediction for sustainable manufacturing. In *Berlin: 11th Global Conference on Sustainable Manufacturing*.
- Wolfram Math World. 2013. *Cylindrical Wedge*. Retrieved 20 Oct 2014, from <http://mathworld.wolfram.com/CylindricalWedge.html>.
- Zhu, K., Y. Wong, and G. Hong. 2009. Multi-category micro-milling tool wear monitoring with continuous hidden Markov models. *Mechanical Systems and Signal Processing* 23: 547–560.